

XUV-laser excitation of molecular fluorine

P.F. Levelt, K.S.E. Eikema, S. Stolte, W. Hogervorst and W. Ubachs

Laser Centre, Vrije Universiteit, De Boelelaan 1081, 1081 HV Amsterdam, The Netherlands

Received 29 March 1993

Excited states of the F_2 molecule are investigated in high resolution by means of 1 XUV+1 UV resonance-enhanced photo-ionization. Perturbations in the $C^1\Sigma_u^+$ valence state and the spectroscopy of the $H^1\Pi_u$ Rydberg state are studied in detail. It is shown that F_2 molecules may be state-selectively detected with a sensitivity of 5×10^7 particles per cm^3 .

1. Introduction

Although fluorine is the simplest halogen molecule its spectrum is not as extensively studied as that of chlorine, bromine and, in particular, iodine. While I_2 has important band systems in the visible, the electronic structure of F_2 is such that absorption on transitions to bound states only occurs at wavelengths shorter than 102 nm. Relatively weak continuous absorption was observed in the near-UV at around 300 nm [1]. Emission in the visible range was recorded as early as 1924 [2], but a determination of term energies of the electronic levels involved had to await data on absorption. Investigations of the discrete absorption spectrum started in 1959 [3]. The most detailed and accurate study of the extreme ultraviolet (XUV) absorption spectrum was reported by Colbourn et al. [4]. In the wavelength range between 95 and 102 nm they observed several vibrational progressions, the most intense being denoted as the $C^1\Sigma_u^+$ state. Vibrational energy spacings indicate a large internuclear equilibrium distance for these states with almost purely ionic binding at large distances. Because of small Franck-Condon overlap factors for transitions to low vibrational levels of the $C^1\Sigma_u^+$ state, this vibrational sequence could not be followed to the bottom of the potential well and vibrational quantum numbers could not be given. In the wavelength range 92–95 nm Colbourn et al. located in addition a Rydberg state denoted as $H^1\Pi_u$ with a characteristic small equilibrium bond distance. Photo-ionization studies

have been performed by Berkowitz et al. [5], who established values for the ionization potential, the dissociation limit of the F_2^+ ion and the limit for ion-pair formation. A theoretical study on the electronic structure of F_2 and F_2^+ was performed by Cartwright and Hay [6].

Laser excitation of molecular fluorine has been applied by Bischel and co-workers [7,8], employing various resonance-enhanced multi-photon ionization (REMPI) techniques. States of gerade symmetry, $F^1\Pi_g$ and $f^3\Pi_g$ were investigated by 2+1 REMPI, while states of ungerade symmetry, the $H^1\Pi_u$ and $h^3\Pi_u$ states, were probed with 3+1 REMPI. In the present study narrow-band XUV-laser radiation is applied in a 1 XUV+1 UV excitation process in F_2 . In contrast to the 3+1 scheme, not only Rydberg states but also valence states, most notably the $C^1\Sigma_u^+$ state, are probed. Limited wavelength regions, covering the $H^1\Pi_u$, $\nu=0, 1$ and 2 states and the $C^1\Sigma_u^+$ vibrational progression near 96 nm, are studied spectroscopically with improved resolution. Moreover it is shown that the 1+1 REMPI scheme allows for a high detection sensitivity: F_2 concentrations as low as 5×10^7 molecules per cm^3 can be detected.

2. Experimental

The XUV-laser spectrometer has been described in some detail in a previous report [9,10]. In short the radiation of a Nd:YAG pumped dye laser system

(10 Hz repetition rate) is frequency-doubled and thereupon tripled in a pulsed gas jet. Xenon is used as the non-linear medium in the present study. For the harmonic conversion process lenses with focal lengths of $f=15$ cm or $f=35$ cm are used. The spatially and temporally overlapping XUV and UV beams perpendicularly intersect a skimmed supersonic molecular beam produced with a second pulsed valve. The intersection zone is at a constant distance from the frequency-tripling zone, so that XUV and UV power densities depend on the choice of the lens. To prevent clogging of the nozzle and corrosion of the equipment the fluorine gas is diluted with He with a ratio 10% F_2 :90% He. A low-density molecular beam from an expansion with a 1 bar backing pressure is used. F_2 spectra are thus recorded from a molecular beam with a partial pressure of 5×10^{-6} Torr in the interaction zone. Adjustment of the nozzle-skimmer distance and the time delay between the opening of the valve and the laser pulse allows for measurements in a relatively hot molecular beam (i.e. 250 K), which is favorable for a spectroscopic study including states with high J quantum numbers.

XUV-laser excitation spectra are recorded by means of 1 XUV + 1 UV photo-ionization. After resonant excitation of F_2 into a particular state by XUV photons the molecules are subsequently ionized by UV photons, which are present in abundance. The ions produced are extracted from the interaction region with a static electric field of about 50 V/cm. In a field-free time-of-flight tube mass separation takes place before detection of the charged particles with an electron multiplier. Ions at selected masses are detected with a boxcar integrator. This wavelength and mass-selective spectroscopic method enables the recording of contamination-free spectra of F_2 , although absorption of N_2 and O_2 rest gas molecules occurs simultaneously. In addition to F_2^+ parent ions also F^+ ions are observed with a relative signal intensity of about 5%–20% (see below).

Excitation spectra are frequency-calibrated by simultaneous recording of an I_2 absorption spectrum at the fundamental wavelength of the dye laser [11]. Spectral line positions in the XUV domain are calibrated with an absolute accuracy of 0.1 cm^{-1} by computerized interpolation. The observed spectral linewidths of 0.3 cm^{-1} are solely determined by the bandwidth of the XUV radiation. The fluorine mol-

ecules are irradiated with XUV intensities estimated of several nJ/pulse, and with UV intensities up to 30 mJ/pulse (in a 5 ns pulse). Pulse-to-pulse fluctuations in the signal intensities of 30% are observed. Spectra are recorded by averaging over 10 shots per wavelength setting.

3. Measurements and interpretation

3.1. Spectroscopy

In fig. 1 an overview of an XUV-laser excitation spectrum of fluorine in the wavelength interval 94.58–97.15 nm, recorded by detection of F_2^+ ions, is shown. The range corresponds to the typical sextupled output of a pulsed dye laser, in this case with a mixture of rhodamine 590 and rhodamine 610, while scanning over its gain profile. The spectrum consists of a vibrational progression of red-shaded bands to the $C^1\Sigma_u^+$ valence state in the notation of Colbourn et al. [4]. The vibrational numbering is not yet established and is therefore given with an arbitrary offset n . The transition to the $C^1\Sigma_u^+$, $v=n+26$ state is strongest and individual spectral lines are recorded with a signal-to-noise ratio of up to 1000. The decreasing signal intensity for transitions to $C^1\Sigma_u^+$, $v < n+26$ states in the range 96.25–97.15 reflects the fact that this part is recorded in the low-output wing of the dye gain profile. The lower signal intensities of the $C^1\Sigma_u^+$, $v > n+26$ bands at the short-wavelength side, between 94.58 and 96.0 nm, correspond to a real decrease and cannot be ascribed to low dye-laser output.

At the short-wavelength side of the recorded spectrum, at $\lambda=94.65$ nm, a blue-shaded band is observed. It shows the typical signature of a Rydberg state with an equilibrium internuclear distance smaller than the ground state. Transitions to the three lowest vibrational levels of this Rydberg state, denoted as $H^1\Pi_u$, are recorded in more detail and line positions determined. A spectrum of the $H^1\Pi_u$ – $X^1\Sigma_g^+$ (1, 0) band is presented in fig. 2. The R branch in the spectra of these three bands is clearly resolved for all J states. Spectroscopic constants for the $H^1\Pi_u$ $v=0$ –2 states are deduced from least-squares fits using energy expressions for the excited state,

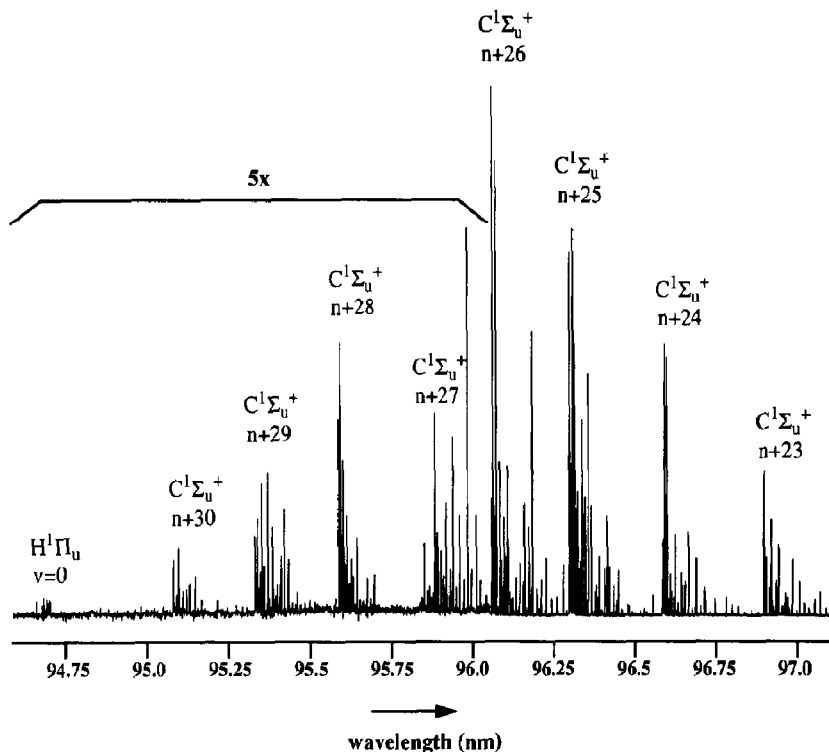


Fig. 1. Overview F_2 spectrum in the wavelength range 94.58–97.15 nm. Part of the vibrational progression of transitions to the $C^1\Sigma_u^+$ valence state as well as the $H^1\Pi_u$ $v=0$ state is shown.

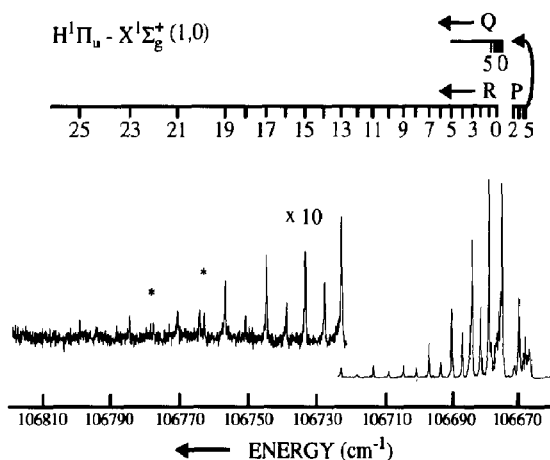


Fig. 2. Spectrum of the $H^1\Pi_u - X^1\Sigma_u^+$ (1,0) transition. The peaks denoted with an asterisk indicate perturbations in the R-branch sequence.

$$E_{\Pi_r}(J) = \nu_0 + BJ(J+1) - DJ^2(J+1)^2 + q_{\Pi}J(J+1), \quad (1)$$

$$E_{\Pi_e}(J) = \nu_0 + BJ(J+1) - DJ^2(J+1)^2. \quad (2)$$

Here ν_0 is the position of the bandhead, B the rotational constant, D the centrifugal distortion parameter and J the rotational quantum number. The subscripts e and f refer to the common convention of electronic symmetry of the two non-degenerate $\Pi(J)$ levels, probed in the Q branch, and the P and R branch respectively. The constants derived from a least-squares minimization routine are listed in table 1. A significant value for the A -doubling constant q_{Π} could only be determined for the $H^1\Pi_u$ $v=1$ state. In the analysis the level energies of the $X^1\Sigma_g^+$ $v=0$ ground state were calculated using the accurate rotational constants of Edwards et al. [12], obtained from Raman spectroscopy: $B_0 = 0.88331 \text{ cm}^{-1}$ and $D_0 = 3.48 \times 10^{-6} \text{ cm}^{-1}$. The observed line positions coincide with the calculated values within the error

Table 1

Spectroscopic constants for the $H^1\Pi_u, v=0-2$ states of F_2 . All values are in cm^{-1}

	$H^1\Pi_u, v=0$	$H^1\Pi_u, v=1$	$H^1\Pi_u, v=2$
ν_0	105606.41(2)	106674.82(2)	107723.33(2)
B	1.0087(5)	0.9976(4)	0.9788(7)
q		-0.0041(5)	

margin of 0.1 cm^{-1} , except for the R(20) and R(22) lines in the (1, 0) band that split into two components, probably as a result of a perturbation with a yet unknown state.

Because the transitions to the $C^1\Sigma_u^+, v=n+25$ and $v=n+26$ states are strongest in intensity, they might provide a suitable and efficient scheme for state-se-

lective probing of F_2 molecules. For this reason detailed measurements on the P and R branches of two bands were performed in order to clarify the spectroscopy. In fig. 3 recordings of the $C^1\Sigma_u^+ - X^1\Sigma_g^+$ ($n+26, 0$) band are presented, for F_2^+ as well as F^+ detection. From the analysis of Colbourn et al. [4] it was established that the $C^1\Sigma_u^+, v=n+26$ state is perturbed by a vibrational level of another $^1\Sigma_u^+$ state, denoted $D^1\Sigma_u^+, v=m+31$. Because of the high spectroscopic precision of the present work (absolute accuracy of 0.1 cm^{-1}) their deperturbation procedure is repeated and extended. In the analysis rotational levels of the $D^1\Sigma_u^+, v=m+31$ and $v=m+32$ are included and excited state energies are calculated by diagonalizing the energy matrix,

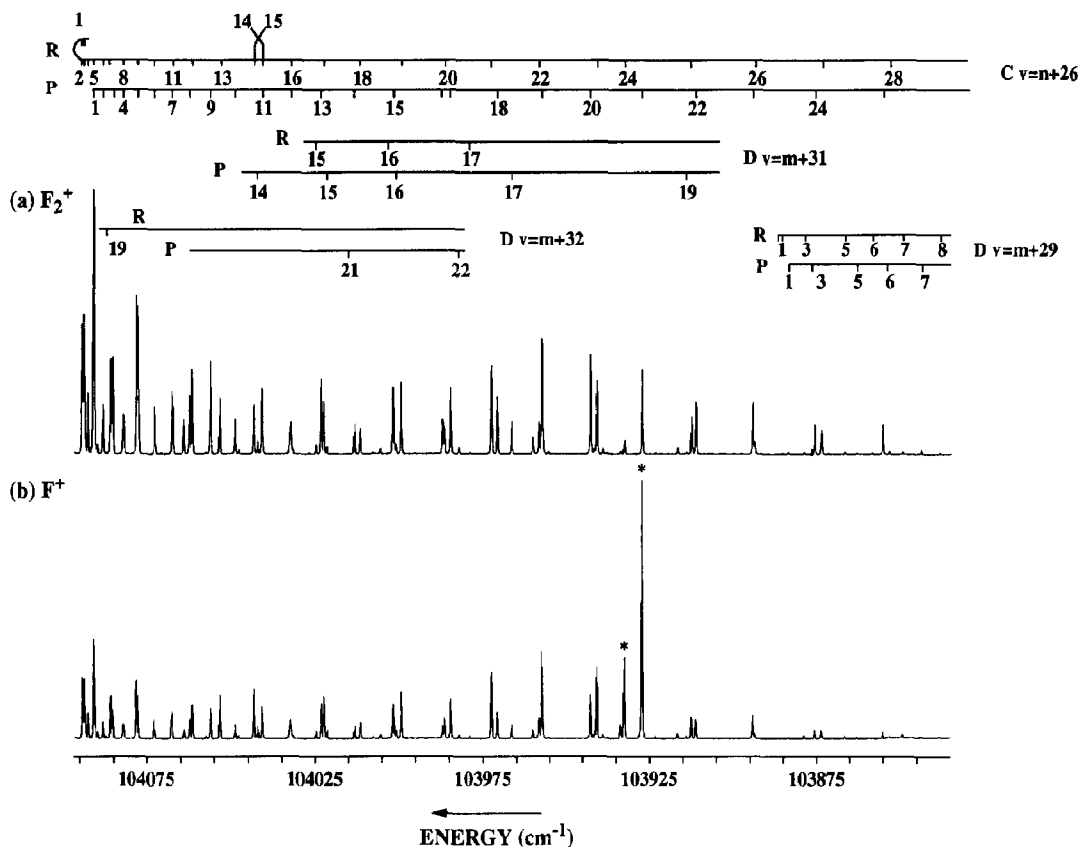


Fig. 3. The $C^1\Sigma_u^+ (v=n+26) - X^1\Sigma_g^+ (v=0)$ transition in F_2 . In the upper trace F_2^+ is detected, in the lower trace F^+ . Notice that as a result of a perturbation the sequence in the R branch is reversed at $J=15$. Transitions to the perturber states $D^1\Sigma_u^+ (v=m+31)$ and ($v=m+32$), made possible by intensity borrowing, are shown as well. The weak bandhead of the $D^1\Sigma_u^+ (v=m+29)$ appears at the low-energy side. The lines marked with an asterisk have an anomalously high F^+ yield.

$$\begin{pmatrix} E_{Cn+26}(J) & H_{CD31} & H_{CD32} \\ H_{CD31} & E_{Dm+31}(J) & 0 \\ H_{CD32} & 0 & E_{Dm+32}(J) \end{pmatrix},$$

for each value of the rotational quantum number J . It is assumed that the perturbation parameters H_{CD} are independent of J , as is expected to be the case for homogeneous interactions between electronic states of the same symmetry. Energies of the deperturbed levels are given in the common notation as in expression (2). P(J) and R(J) transitions for the three bands are calculated from the eigenvalues of the matrix. After assignment of the spectral lines the spectroscopic constants and interaction parameters are obtained from a least-squares minimization routine. We could assign the R(0)–R(27) and P(1)–P(26) lines of the C–X ($n+26, 0$) band, the R(15)–R(17) and P(14)–P(19) lines of the D–X ($m+31, 0$) band and the R(19) and P(21)–P(22) lines of the D–X ($m+32, 0$) band. All lines are included in the fit. The resulting parameters are listed in table 2. One of the interactions is clearly visible in the spectrum of fig. 3 as a change of sequence in the R branch of the C–X ($n+26, 0$) band at R(14)–R(15). The anti-crossing with D, $v=m+31$ takes place between $J=15$ and 16, while D, $v=m+32$ anti-crosses between 24 and 25. The next anti-crossing, with D, $v=m+33$ is expected at $J=29$, but here the data are insufficient

Table 2

Spectroscopic constants of F_2 for the $C^1\Sigma_u^+$ $v=n+25$ and $v=n+26$ states and the perturbing $D^1\Sigma_u^+$ $v=m+29, m+31$ and $m+32$ states as well as the homogeneous perturbation parameters. All values are in cm^{-1}

	$C^1\Sigma_u^+ v=n+25$	$C^1\Sigma_u^+ v=n+26$	
ν_0	103833.16 ± 0.05	104093.09 ± 0.02	
B	0.5175 ± 0.0004	0.6049 ± 0.0002	
D	$(4.73 \pm 0.08) \times 10^{-5}$	$(6.97 \pm 0.04) \times 10^{-5}$	
	$D^1\Sigma_u^+ v=m+29$	$D^1\Sigma_u^+ v=m+31$	$D^1\Sigma_u^+ v=m+32$
ν_0	103885.1 ± 0.1	104196.17 ± 0.1	104357.23 ± 0.1
B	0.1602 ± 0.002	0.1692 ± 0.0004	0.1749 ± 0.0003
D	$(2 \pm 1) \times 10^{-5}$	$(2.8 \pm 0.4) \times 10^{-5}$	$(5.0 \pm 0.1) \times 10^{-5}$
$H[C^1\Sigma_u^+ v=n+25] \times [D^1\Sigma_u^+ v=m+29]$			6.56 ± 0.05
$H[C^1\Sigma_u^+ v=n+26] \times [D^1\Sigma_u^+ v=m+31]$			6.94 ± 0.03
$H[C^1\Sigma_u^+ v=n+26] \times [D^1\Sigma_u^+ v=m+32]$			7.52 ± 0.05

for a detailed analysis. All lines included in the routine fit with a resulting standard deviation of 0.12 cm^{-1} . However, the R(6) and P(8) lines of the C–X ($n+26, 0$) band are both shifted downward in energy by a significant 0.6 cm^{-1} . This is an indication of another perturbation of the C, $v=n+26$ state, albeit a much weaker one than the other two. As the $C^1\Sigma_u^+$, $v=n+26, J=7$ state lies at 104125 cm^{-1} the band origin of the perturbing state is expected near 104115 cm^{-1} assuming a rotational constant of 0.16 cm^{-1} . From interpolation of the vibrational spacing in the $D^1\Sigma_u^+$ states it follows that the $D^1\Sigma_u^+$, $v=m+30$ state cannot cause this perturbation. Its energy is 70 cm^{-1} too low. However, Colbourn et al. observed another vibrational progression, denoted as $E^1\Sigma_u^+$. Extrapolation of the band origins upward from $E^1\Sigma_u^+$, $v=p+17$ indicates that the perturber of the $C^1\Sigma_u^+$, $v=n+26, J=7$ state may well be the $E^1\Sigma_u^+$, $v=p+20, J=7$ state.

The $C^1\Sigma_u^+$, $v=n+25$ state, and a single perturber, the $D^1\Sigma_u^+$, $v=m+29$ state, are treated in a similar procedure and the resulting parameters are also listed in table 2. In this case the anti-crossing occurs between $J=11$ and 12. The bandhead of the D–X ($m+29, 0$) band is observable as weak lines near 103885 cm^{-1} in the spectrum of fig. 3. The signal-to-noise ratio in these lines is about 10, a factor of 100 lower than in the C–X ($n+26, 0$) band.

We note that the intensities of transitions to the perturber states largely depend on the mixing of the excited state eigenfunctions. Where at the bandhead the intensity of the D–X ($m+29, 0$) lines is only 1% of the intensity of the C–X lines, the R(11) line of the D–X ($m+29, 0$) band has 60% of the intensity of the R(11) line of the C–X ($n+25, 0$) band. At $J=12$ the $Cn+25$ state has 61% C-state character, while the $Dm+29$ state has 39% C-state character. The intensities of transitions to all $D^1\Sigma_u^+$, v, J perturber states is quantitatively analyzed and it is found that they are also determined by the C-state character of the excited state.

3.2. F_2^+ parent ion and F^+ fragment ion formation

Molecular fluorine excitation spectra have been measured by simultaneous recording of signals de-

ferent routes that may lead to fragment ion formation indicated. In view of the intensity ratios of XUV and UV laser beams (UV 10^6 more intense) it is unlikely that a second XUV photon will be absorbed.

The first possible channel is that of ion-pair formation after excitation of a doubly excited intermediate state. The energy threshold for ion-pair formation is 15.58 eV [5], which is reached by absorption of an XUV photon and a single UV photon. So the ion-pair channel requires the same number of UV photons as the parent-ion channel. The fact that F^+ production more strongly depends on UV intensity is an argument against the ion-pair hypothesis.

The second channel for F^+ formation, the dissociation of the F_2^+ parent ion, requires absorption of an additional UV photon. Energetically 19.01 eV is needed for the process $F_2 \rightarrow F^+ + F$ and this is provided by 1 XUV plus 2 UV photons. From the study of Cartwright and Hay [6] it follows that an F_2^+ ion in the $X^2\Pi_g$ ground state may be vertically excited to the repulsive part of the first $^2\Pi_u$ state by a 4 eV photon. So this channel can well explain the steeper UV dependence for F^+ formation. The excitation to a repulsive state indicates a non-resonance behaviour in the ionic absorption as well. This explains why the relative intensities of the F^+ yield closely follow those of the F_2^+ yield.

In the third channel after resonant absorption of an XUV photon the neutral molecules are further excited by absorption of a UV photon into a doubly excited state F_2^{**} , that may dissociate into a ground state neutral atom and an excited neutral atom, denoted by F^* . If the dissociation energy of F_2 is accounted for (1.59 eV [5]), via this process only atomic states of the $(2s)^2(2p)^43s$ configuration may be populated. The excited atom may absorb further UV photons, first into a Rydberg state (F^{**}) just below the atomic ionization threshold, followed by a second one producing F^+ . In the sequence of channel (3) in two of the steps coincidental UV wavelength-dependent excitation is supposed. Therefore this route might explain the coincidental anomalies in the F^+ yield. However, the structure of the doubly excited molecular states (F_2^{**}) as well as the atomic Rydberg states (F^{**}) is not known, so no definite conclusions may be drawn. It seems certain that channel (3) cannot provide an explanation for the

major part of the F^+ yield, that follows the intensity pattern of the F_2^+ yield.

As a fourth route atomic excitation by XUV photons might be considered. The UV intensity is such that 0.1% of F_2 is dissociated during the laser pulse [1]. Ground state F atoms subsequently may be ionized in a 1 XUV+2 UV REMPI process analogous to the 3+2 REMPI excitations observed by Bischel and Jusinski [7]. In that case resonances are expected at wavelengths of 95.48, 95.19, 95.55 and 95.15 nm corresponding to transitions in the F atom [13]. However these atomic resonances are not observed.

It is concluded that channel (2), dissociative UV excitation of the F_2^+ parent ion, is the most probable route for the formation of F^+ , at least for the vast majority of features. The resonance features with anomalously high F^+ yield may be interpreted as related to channel (3), where excited state F atoms are photo-ionized.

4. Conclusion and outlook

The method of 1 XUV+1 UV photoionization is shown to be a highly sensitive spectroscopic tool for the study of excited states of F_2 with high resolution. As an example the perturbations in the spectra of two selected valence bands of the $C^1\Sigma_u^+$ state were treated in detail. Furthermore accurate spectroscopic constants could be determined for the $H^1\Pi_u$ $v=0-2$ states. In principle the present apparatus may be used for a study of the full wavelength range 90–102 nm.

The band intensities observed in the present study markedly differ from those obtained in 3+1 REMPI studies of Bischel et al. [7,8]. In those experiments, performed in a geometry with a focused UV-laser beam, the $H^1\Pi_u$ and $h^3\Pi_u$ Rydberg states were observed and no evidence of the $C^1\Sigma_u^+$ state was found. In agreement with observations of Colbourn et al. [4], it is found that the intensities of transitions to the $D^1\Sigma_u^+$ state are governed by intensity borrowing from the $C^1\Sigma_u^+$ state. While this was found to hold for whole bands at low vibrational levels, strong J -dependent intensity borrowing effects within a particular band are observed in the present work. No direct evidence of the $E^1\Sigma_u^+$ state is observed, other

than an indirect indication of a perturbation with the $C^1\Sigma_u^+$ state.

The spectra of F_2 have been recorded in a diluted, low-pressure molecular beam expansion with a relatively high rotational temperature. Assuming an F_2 particle density of about $5 \times 10^{10} \text{ cm}^{-3}$ in the interaction zone, taking into account a distribution over rotational quantum states and a signal-to-noise ratio of 1000, a detection limit of 5×10^7 molecules per cm^3 or 5×10^6 molecules per quantum state per cm^3 is estimated. This implies that a 1 XUV + 1 UV photoionization scheme is a sensitive tool for the state-selective detection of F_2 molecules. This method may prove fruitful in various applications, such as in gas-phase reaction dynamics and surface scattering experiments involving F_2 (e.g. etching).

Acknowledgement

The authors are grateful to J. Bouma for his skillful technical support in the construction of the XUV-laser spectrometer. This work was financially supported by the Foundation of Fundamental Research of Matter (FOM), which is part of the Netherlands

Organisation for Scientific Research (NWO).

References

- [1] R. Holland and J.L. Lyman, *J. Quant. Spectry. Radiative Transfer* 38 (1987) 79.
- [2] H.G. Gale and G.S. Monk, *Astrophys. J.* 59 (1924) 125; 69 (1929) 77.
- [3] R.P. Iczkowski and J.L. Margrave, *J. Chem. Phys.* 30 (1959) 403.
- [4] E.A. Colbourn, M. Dagenais, A.E. Douglas and J.W. Raymonda, *Can. J. Phys.* 54 (1976) 1343.
- [5] J. Berkowitz, W.A. Chupka, P.M. Guyon, J.H. Holloway and R. Spohr, *J. Chem. Phys.* 54 (1971) 5165.
- [6] D.C. Cartwright and P.J. Hay, *Chem. Phys.* 114 (1987) 305.
- [7] W.K. Bischel and L.E. Jusinski, *Chem. Phys. Letters* 120 (1985) 337.
- [8] G.W. Faris, M.J. Dyer, D.L. Huestis and W.K. Bischel, *J. Chem. Phys.* 97 (1992) 5964.
- [9] P.F. Levelt and W. Ubachs, *Chem. Phys.* 163 (1992) 263.
- [10] P.F. Levelt, W. Ubachs and W. Hogervorst, *J. Chem. Phys.* 79 (1992) 7160.
- [11] S. Gerstenkorn and P. Luc, *Atlas du spectre d'absorption de la moleculle de l'iode entre 14800–20000 cm^{-1}* (Editions du CNRS, Paris, 1978).
- [12] H.G.M. Edwards, E.A.M. Good and D.A. Long, *J. Chem. Soc. Faraday Trans. II* 72 (1975) 984.
- [13] C.E. Moore, *Atomic energy levels*, Vol. 1, NSRDS-NBS (US GPO, Washington, 1971) p. 60.